We are IntechOpen,
the world's leading publisher of
Open Access books
Built by scientists, for scientists

6,900
Open access books available

186,000
International authors and editors

200M
Downloads

Our authors are among the

154
Countries delivered to

TOP 1%
most cited scientists

12.2%
Contributors from top 500 universities

CLARIVATE ANALYTICS
BOOK CITATION INDEX
INDEXED

WEB OF SCIENCE™

Selection of our books indexed in the Book Citation Index
in Web of Science™ Core Collection (BKCI)

Interested in publishing with us?
Contact book.department@intechopen.com

Numbers displayed above are based on latest data collected.
For more information visit www.intechopen.com

EIT-Based Photonic Crystals and Photonic Logic Gate Design

Teh-Chau Liau[1], Jin-Jei Wu[2], Jian Qi Shen[3] and Tzong-Jer Yang[2]
[1]Ph. D. Program in Engineering Science, College of Engineering
Chung Hua University, Hsinchu, Taiwan
[2]Department of Electrical Engineering, Chung Hua University, Hsinchu, Taiwan
[3]Centre for Optical and Electromagnetic Research, State Key Laboratory of
Modern Optical Instrumentations,
Zijingang Campus, Zhejiang University, Hangzhou
China

1. Introduction

Over the past two decades, the effects of atomic phase coherence have exhibited a number of physically interesting phenomena such as electromagnetically induced transparency (EIT) (Harris, 1997) and the effects that are relevant to EIT, including light amplification without inversion (Cohen & Berman, 1997), spontaneous emission cancellation (Zhu & Scully, 1996), multi-photon population trapping (Champenois et al., 2006), coherent phase control (Zheltikov, 2006; Gandman et al., 2007) as well as photonic resonant left-handed media (Krowne & Shen, 2009). EIT is such a quantum optical phenomenon that if one resonant laser beam propagates in a medium (e.g., an atomic vapor or a semiconductor-quantum-dot material), the beam will get absorbed; but if two resonant laser beams instead propagate inside the same medium, neither would be absorbed. Thus the opaque medium becomes a transparent one. Such an interesting optical behavior would lead to many applications, e.g., designs of new photonic and quantum optical devices. Since it can exhibit many intriguing optical properties and effects, EIT has attracted extensive attentions of a large number of researchers in a variety of areas of optics, atomic physics and condensed state physics (Harris, 1997), and this enables physicists to achieve new novel theoretical and experimental results. For example, some unusual physical effects associated with EIT include the ultraslow light pulse propagation, the superluminal light propagation, and the light storage in atomic vapors (Schmidt & Imamoğlu, 1996; Wang et al., 2000; Arve, 2004; Shen et al., 2004), some of which are expected to be beneficial (and powerful) for developing new technologies in quantum optics and photonics.

In this chapter, we shall consider a new application of EIT, i.e., EIT-based artificial periodic dielectric: specifically, the EIT medium (an atomic vapor or a semiconductor-quantum-dot material) is embedded in a periodic host dielectric (e.g., GaAs). As is well known, the photonic crystals, which are periodic arrangements of dielectrics, have captured wide attention in physics, materials science and other relevant fields (e.g., information science)

due to its capacity of controlling light propagations (Yablonovitch, 1987; Joannopoulos et al., 1995; Joannopoulos et al., 1997). Here, we shall propose some new effects relevant to light propagation manipulation via EIT responses in an artificial periodic dielectric. Such effects result from the combination of EIT and photonic crystals. In this new application of EIT for manipulating light wave propagations, the periodic dielectric can exhibit a tunable reflectance and transmittance (induced by an external control field) and can show extraordinary sensitivity to the frequency of the applied probe field. For example, a change of one part in 10^8 in the probe frequency ω_p would lead to a dramatic change in the reflectance and transmittance of the EIT-based periodic layered medium, and therefore, it can be used for designing sensitive optical switches, photonic logic gates as well as tunable photonic transistors. In the literature, although there have been some investigations that are relevant to the tunable photonic crystals based on EIT media (Forsberg & She, 2006; He et al., 2006; Zhuang et al., 2007; Petrosyan, 2007), yet less attention has been paid to the frequency-sensitive optical behavior that would be the most remarkable property of such a kind of periodic layered media.

We should point out that photonic logic gates designed based on new coherent materials, such as near-field optically coupled nanometric materials (Sangu et al., 2004; Kawazoe et al., 2003) and double-control multilevel atomic media (Shen, 2007; Shen & Zhang, 2007; Gharibi et al., 2009), have been suggested during the past few years. It should be emphasized that the mechanism presented in this chapter can be considered an alternative way to realize such a kind of photonic and quantum optical devices. Very recently, Abdumalikov et al. reported an experimental observation of EIT on a single artificial atom, and found that the propagating electromagnetic waves are allowed to be fully transmitted or backscattered (Abdumalikov et al., 2010). We will demonstrate in the present chapter that such a full controllability of optical property of artificial media could also be achieved in the EIT-based layered structure, of which the reflectance can be either zero or large depending sensitively on the intensity of the external control field applied in the EIT system. We believe that this would open a good perspective for its application in some new fields such as photonic microcircuits (or integrated optical circuits).

This chapter is organized as follows. In Sec. 2 we shall discuss the characteristic optical property of an EIT medium (e.g., an atomic vapor), and in Sec. 3 we review a formulation for treating the electromagnetic wave propagation in a periodic layered medium. The frequency-sensitive tunable band structure as well as the behavior of frequency-sensitive reflectance and transmittance of such an EIT-based periodic layered medium are presented in Sec. 4 and Sec. 5, respectively, where the spectrum of the reflectance as well as the transmittance of the EIT-based periodic structure (when the TE wave of the probe beam is normally incident on the layered medium) versus the normalized Rabi frequency Ω_c / Γ_3 of the control field and the normalized probe frequency detuning Δ_p / Γ_3 will be addressed. The frequency-sensitive tunable band structure of TM wave in the EIT-based periodic structure containing a left-handed medium is discussed in Sec. 6, where the reflection coefficient exceeding unity would occur in some frequency ranges. This will lead to a negative transmittance (so-called photonic analog of Klein tunneling in an LHM-EIT-based periodic layered medium). In Sec. 7 and Sec. 8, a potential application, i.e., photonic transistors and logic gates (tunable photonic logic gates) are suggested by taking full

advantage of the effect of such an optical switching control. In Sec. 9 we close the chapter with some concluding remarks.

2. Optical properties of an EIT medium

Here we shall address the intriguing optical behavior of an EIT atomic vapor. Consider a Lambda-configuration three-level atomic system with two lower levels $|1\rangle$, $|2\rangle$ and one upper level $|3\rangle$ (see Fig.1 for its schematic diagram). This atomic system interacts with the electric fields of the two applied light waves (probe and control fields), which drive the $|1\rangle$-$|3\rangle$ and $|2\rangle$-$|3\rangle$ transitions, respectively. Note that the parity of level $|3\rangle$ needs to be opposite to levels $|1\rangle$ and $|2\rangle$, since the level pairs $|1\rangle$-$|3\rangle$ and $|2\rangle$-$|3\rangle$ can be coupled to the electric fields of the probe and control waves, respectively. Such a three-level system can be found in metallic alkali atoms (e.g., Na, K, and Rb). The off-diagonal density matrix elements ρ_{21} and ρ_{31} can form a closed set of equations under the condition of weak probe field (Scully & Zubairy, 1997), and the atomic system can be characterized by an SU(2) time-dependent model when the control field intensity varies adiabatically. The present atomic system interacting with two light fields (Ω_c and Ω_p) is governed by

$$\frac{\partial}{\partial t}\begin{pmatrix} \rho_{21} \\ \rho_{31} \end{pmatrix} = \begin{pmatrix} -\left[\dfrac{\gamma_2}{2}+i\left(\Delta_p-\Delta_c\right)\right] & \dfrac{i}{2}\Omega_c^* \\ \dfrac{i}{2}\Omega_c & -\left(\dfrac{\Gamma_3}{2}+i\Delta_p\right) \end{pmatrix}\begin{pmatrix} \rho_{21} \\ \rho_{31} \end{pmatrix} + \begin{pmatrix} 0 \\ \dfrac{i}{2}\Omega_p \end{pmatrix}. \tag{1}$$

It can be verified that the atomic microscopic electric polarizability of the $|1\rangle$-$|3\rangle$ transition is of the form

$$\beta = \frac{i\,|\wp_{13}|^2}{\varepsilon_0\hbar}\frac{\dfrac{\gamma_2}{2}+i\left(\Delta_p-\Delta_c\right)}{\left(\dfrac{\Gamma_3}{2}+i\Delta_p\right)\left[\dfrac{\gamma_2}{2}+i\left(\Delta_p-\Delta_c\right)\right]+\dfrac{1}{4}\Omega_c^*\Omega_c}. \tag{2}$$

Here, Γ_3 and γ_2 stand for the spontaneous emission decay rate and the collisional dephasing rate, respectively. The Rabi frequency Ω_c of the control field is defined by $\Omega_c = \wp_{32}E_c/\hbar$ with E_c the slowly-varying amplitude (envelope) of the control field. The two frequency detunings are defined as $\Delta_p = \omega_{31}-\omega_p$, $\Delta_c = \omega_{32}-\omega_c$ with ω_p and ω_c the mode frequencies of the probe field and the control field, respectively. By using the Clausius-Mossotti relation (governing the local field effect due to the dipole-dipole interaction between neighboring atoms), the relative electric permittivity of the EIT vapor at probe frequency ($\omega_p = \omega_{31}-\Delta_p$) is given by

$$\varepsilon_r = 1 + \frac{N_a\beta}{1-\dfrac{N_a\beta}{3}}, \tag{3}$$

where N_a denotes the atomic concentration (atomic number per unit volume) of the EIT atomic vapor.
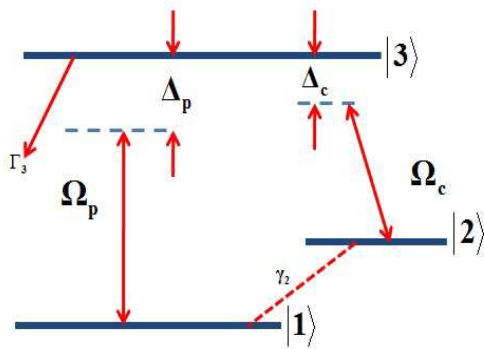
Fig. 1. The schematic diagram of a three-level EIT atomic system. The parity of upper level $|3\rangle$ is opposite to that of lower levels $|1\rangle$ and $|2\rangle$. The control and probe laser beams drive the $|2\rangle$-$|3\rangle$ and $|1\rangle$-$|3\rangle$ transitions, respectively. Once the control laser beam Ω_c is switched off, the vapor will be a resonantly absorptive medium for the probe light. However, the vapor would be transparent to the probe light because of the destructive quantum interference between the $|1\rangle$-$|3\rangle$ and $|2\rangle$-$|3\rangle$ transitions when the control laser beam is present.

The tunable dispersive behavior of the bulk EIT atomic vapor is shown in Figs. 2 and 3. The typical atomic and optical parameters chosen for Figs. 2 and 3 are as follows: the atomic number density $N_a = 5.0 \times 10^{20}$ m^{-3}, the electrical dipole moment $|\wp_{31}| = 1.0 \times 10^{-29}$ C·m, the frequency detuning of the control field $\Delta_c = 1.0 \times 10^7$ s^{-1}, the spontaneous emission decay rate $\Gamma_3 = 2.0 \times 10^7$ s^{-1} and the dephasing rate $\gamma_2 = 1.0 \times 10^5$ s^{-1}. Fig. 3 shows the three-dimensional behavior of the real part (a) and the imaginary part (b) of the relative electric permittivity of the EIT atomic vapor (bulk). As the dispersive curve of the refractive index of the EIT bulk is a function of Δ_p and Ω_c, in the section that follows, we shall consider a band structure (versus both Δ_p and Ω_c) of the EIT-based periodic medium (see Fig. 4 for its schematic diagram).
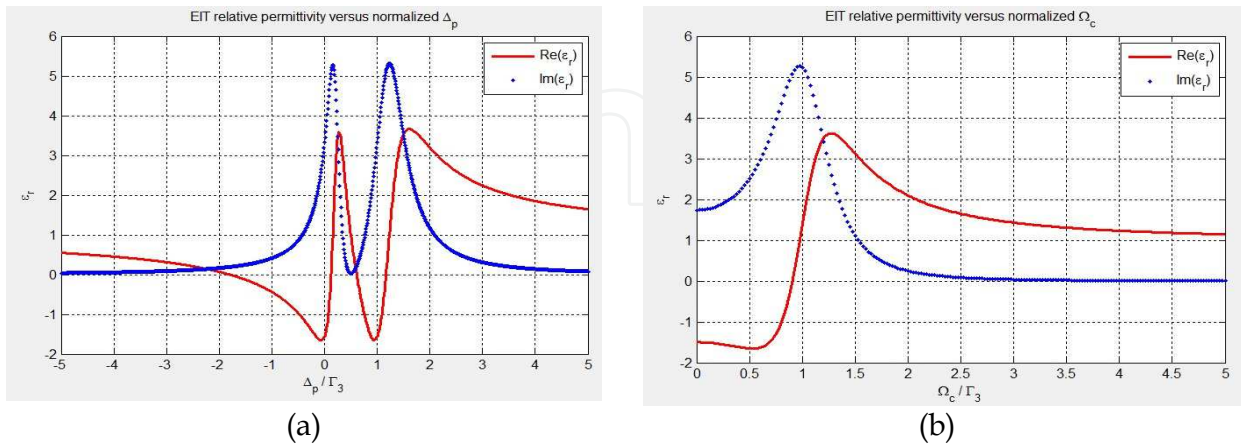

| (a) | (b) |

Fig. 2. The relative electric permittivity of the three-level EIT atomic vapor as a function of the probe frequency detuning Δ_p and the Rabi frequency Ω_c of the control field. In (a) the Rabi frequency of the control field is $\Omega_c = 2.0 \times 10^7$ s^{-1}. In (b) the probe frequency detuning is $\Delta_p = 3.4 \times 10^6$ s^{-1}.
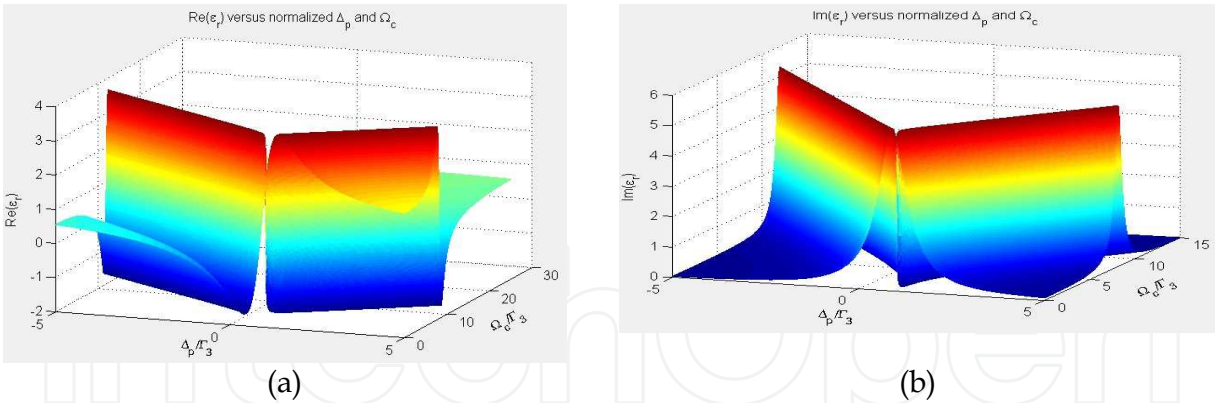
Fig. 3. The dispersion of the relative electric permittivity of the EIT atomic medium versus the frequency detuning Δ_p of the probe field and the Rabi frequency Ω_c of the control field.

The 1D periodic (D|E) cells shown in Fig. 4 are composed of two kinds of media: a dielectric (e.g., GaAs dielectric with the relative refractive index $n_1 = 3.54$) and a typical Lambda-configuration three-level EIT medium whose electric permittivity is determined by Eqs. (2) and (3). Here, the characters "D" and "E" in "(D|E)" denote the dielectric (GaAs) and the EIT, respectively. Assume the two materials are both homogeneous along y-direction (i.e. $\partial/\partial y = 0$) and the probe signal wave travels in the $(...D|E|D|E...)$ structure always along x-direction. The reflection coefficient (Yeh, 2005) on the left side interface ($x=0$) of such an EIT-based periodic medium, which is in fact a 1D N-layer (D|E) layered structure bounded by the GaAs dielectric material, will be addressed.
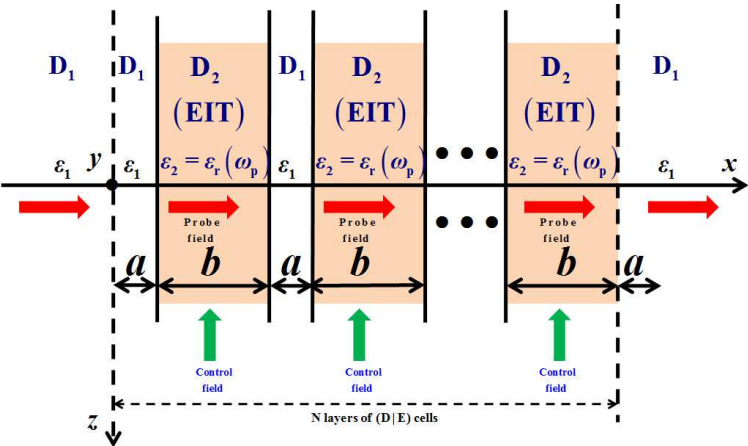

Fig. 4. The 1D N-layer structure of (D|E) cells embedded in GaAs homogeneous dielectric. The dielectrics D_1 and D_2 stand for the GaAs and EIT atomic media, respectively. A (D|E) cell consists of GaAs dielectric (D) and EIT medium (E). The lattice constants of the (D|E) cells are chosen as $a = b = 0.1\mu m$.

3. The electromagnetism of periodic layered medium

In order to make the chapter self-contained, we shall in this section review the formalism for treating the light wave propagation in a periodic layered medium (Readers are referred to e.g. Yeh's reference (Yeh, 2005) for a more complete and detailed formalism). According to

the theory of electromagnetism in photonic crystals, the electric field in the mth unit cell can be expressed by (Yeh, 2005)

$$E(x) = \begin{cases} a_m e^{-jk_{1x}(x-m\Lambda)} + b_m e^{jk_{1x}(x-m\Lambda)}, & m\Lambda - a < x < m\Lambda \\ c_m e^{-jk_{2x}(x-m\Lambda+a)} + d_m e^{jk_{2x}(x-m\Lambda+a)}. & (m-1)\Lambda < x < m\Lambda - a \end{cases} \tag{4}$$

Here, the wave vectors $k_{1x} = n_1\omega/c$, $k_{2x} = n_2\omega/c$. By using the matrix formalism for treating the wave propagation in layered media, one can arrive at the equation

$$\begin{pmatrix} a_{m-1} \\ b_{m-1} \end{pmatrix} = \frac{1}{2} \begin{pmatrix} e^{jk_{2x}b}\left(1+\dfrac{k_{2x}}{k_{1x}}\right) & e^{-jk_{2x}b}\left(1-\dfrac{k_{2x}}{k_{1x}}\right) \\ e^{jk_{2x}b}\left(1-\dfrac{k_{2x}}{k_{1x}}\right) & e^{-jk_{2x}b}\left(1+\dfrac{k_{2x}}{k_{1x}}\right) \end{pmatrix} \begin{pmatrix} c_m \\ d_m \end{pmatrix} \tag{5}$$

of electric field amplitudes as well as the eigenvalue equation

$$\begin{pmatrix} A & B \\ C & D \end{pmatrix} \begin{pmatrix} a_m \\ b_m \end{pmatrix} = e^{iK\Lambda} \begin{pmatrix} a_m \\ b_m \end{pmatrix} \tag{6}$$

for the column vector characterizing the electromagnetic field strengths in the periodic layered structure. The matrix elements are given by (Yeh, 2005)

$$A = e^{jk_{1x}a}\left[\cos k_{2x}b + \frac{1}{2}j\left(\frac{k_{2x}}{k_{1x}} + \frac{k_{1x}}{k_{2x}}\right)\sin k_{2x}b\right],$$
$$B = e^{-jk_{1x}a}\left[\frac{1}{2}j\left(\frac{k_{2x}}{k_{1x}} - \frac{k_{1x}}{k_{2x}}\right)\sin k_{2x}b\right], \tag{7a}$$

$$C = e^{jk_{1x}a}\left[-\frac{1}{2}j\left(\frac{k_{2x}}{k_{1x}} - \frac{k_{1x}}{k_{2x}}\right)\sin k_{2x}b\right],$$
$$D = e^{-jk_{1x}a}\left[\cos k_{2x}b - \frac{1}{2}j\left(\frac{k_{2x}}{k_{1x}} + \frac{k_{1x}}{k_{2x}}\right)\sin k_{2x}b\right]. \tag{7b}$$

Note that the eigenvalue equation yields

$$\det\begin{pmatrix} A - e^{jK\Lambda} & B \\ C & D - e^{jK\Lambda} \end{pmatrix} = 0. \tag{8}$$

This can be rewritten as a well-known form

$$\cos K\Lambda = \cos k_{1x}a \cos k_{2x}b - \frac{1}{2}\left(\frac{n_2}{n_1} + \frac{n_1}{n_2}\right)\sin k_{1x}a \sin k_{2x}b. \tag{9}$$

From this relation, one can obtain the Bloch wave number K. Now we are in a position to derive the coefficient of reflection, which is defined as $r_N = b_0/a_0$. It follows that the relation

of the column vectors between the left side interface (at $x = 0$) and in the Nth unit cell is given by (Yeh, 2005)

$$\begin{pmatrix} a_0 \\ b_0 \end{pmatrix} = \begin{pmatrix} A & B \\ C & D \end{pmatrix}^N \begin{pmatrix} a_N \\ b_N \end{pmatrix} \quad (10)$$

with

$$\begin{pmatrix} A & B \\ C & D \end{pmatrix}^N = \begin{pmatrix} AU_{N-1} - U_{N-2} & BU_{N-1} \\ CU_{N-1} & DU_{N-1} - U_{N-2} \end{pmatrix}. \quad (11)$$

Here, the explicit expression for U_N is $U_N = \dfrac{\sin\left[(N+1)K\Lambda\right]}{\sin K\Lambda}$. With the help of the relations

$$\begin{aligned} a_0 &= \left(AU_{N-1} - U_{N-2}\right)a_N + BU_{N-1}b_N, \\ b_0 &= CU_{N-1}a_N + \left(DU_{N-1} - U_{N-2}\right)b_N, \end{aligned} \quad (12)$$

the coefficient of reflection of an N -layer periodic medium is given by (Yeh, 2005)

$$r_N = \frac{CU_{N-1}}{AU_{N-1} - U_{N-2}}, \quad (13)$$

where $b_N = 0$ has been substituted (since the present periodic layered medium is composed of N unit cells and is bounded by the medium of the refractive index n_1, the reflected amplitude of the electric field in the last unit cell vanishes). It should be emphasized that the factor of phasor time dependence, $\mathrm{e}^{-\mathrm{i}\omega t}$, has been adopted for the time harmonic wave in deriving the atomic microscopic electric polarizability (2) of EIT. Such a convention is often used by physicists. In the convention of engineers, however, the time dependence is $\mathrm{e}^{+\mathrm{j}\omega t}$ (Yeh, 2005; Caloz & Itoh, 2006). As we shall employ the formalism in the reference of Yeh (Yeh, 2005) for treating the wave propagation in the periodic layered medium, we need to convert the convention of physicists to that of engineers. This can be easily accomplished by the imaginary variable substitution, i.e., $\mathrm{i} \rightarrow -\mathrm{j}$.

In the sections that follow, we shall concentrate our attention on the influence of the external control field on the probe wave propagation inside the EIT-based periodic layered medium. It should be noted that we only consider a passive multilayered structure in this chapter. Although there are control and probe laser beams exciting the two electric-dipole allowed transitions, it is a passive atomic system because of the large spontaneous emission decay from the excited states to the ground state. If, however, there is an extra strong pumping laser beams driving the atomic system (Wu, 2004), we should address its optical response relevant to gain factor. But here such a strong pumping interaction is not taken into account.

4. The frequency-sensitive tunable band structure

In order to show how sensitive (to the probe frequency) the band structure of the EIT photonic crystal is, let us first see the dispersive relation of the 1D infinite periodic (D|E) cells, in which the probe frequency ω_p is far from the resonant frequency of the atomic

$|1\rangle$ - $|3\rangle$ transition. We shall plot the band structure by using Eq. (9), which is an equation of dispersion of a 1D infinite periodic structure. Since the permittivity of EIT also depends upon the Rabi frequency of the control field, $\Omega_{\mathbf{c}}$ is a tunable parameter involved in the equation of dispersion. Then we will also present the three-dimensional behavior of the Bloch wave number versus both $\Omega_{\mathbf{c}}$ and Δ_{p} with the help of Eqs. (2), (3) and (9). Here, we choose the typical atomic transition frequency $\omega_{31} = 5.0 \times 10^{15}$ s^{-1}, and the thickness of the two layers $a = 0.1 \mu$m (GaAs dielectric) and $b = 0.1 \mu$m (EIT medium).

As the probe frequency detuning of TE waves in Fig. 5 is quite large ($\Delta_{\mathrm{p}} \approx \pi c / \Lambda$ with $\Lambda = a + b$), the strong dispersion of EIT cannot be exhibited, and the present (D | E) layered structure behaves like a conventional 1D photonic crystal. However, when the probe frequency detuning Δ_{p} approaches zero (or negligibly small compared with $\pi c / \Lambda$ having the order of magnitude 10^{15} s^{-1}, e.g., Δ_{p} is tuned onto resonance, i.e., $\Delta_{\mathrm{p}} \rightarrow \Delta_{\mathrm{c}}$ that equals 1.0×10^7 s^{-1}), it would exhibit a band with a fine structure (and hence remarkable frequency-sensitive reflectance and transmittance). The band structure in the probe frequency detuning range $\Delta_{\mathbf{p}} / \Gamma_{\mathbf{3}} \in [-2.5 \times 10^8, +2.5 \times 10^8]$ is plotted in Fig. 5 (a). The typical atomic and optical parameters such as the atomic number density $N_{\mathbf{a}}$, the electrical dipole moment $|\wp_{\mathbf{31}}|$, the control frequency detuning $\Delta_{\mathbf{c}}$, the spontaneous emission decay rate $\Gamma_{\mathbf{3}}$ and the dephasing rate $\gamma_{\mathbf{2}}$ are chosen exactly the same as in Figs. 2 and 3 (these typical parameters are also used throughout the chapter). The Rabi frequency of the control field is $\Omega_{\mathbf{c}} = 2.0 \times 10^7$ s^{-1}. Since, seen from Fig. 5 (a), there are some fine structures of the band in the frequency range ($\Delta_{\mathbf{p}} / \Gamma_{\mathbf{3}} \in [-2.5 \times 10^8, +2.5 \times 10^8]$) that need to be addressed, we present the intricate structures in Fig. 5(b)-(d) and demonstrate them in more details. In Fig. 5(b), for example, as the probe frequency detuning tends to the resonant frequency $\Delta_{\mathrm{p}} \rightarrow \Delta_{\mathrm{c}}$ (i.e., $\Delta_{\mathbf{p}} / \Gamma_{\mathbf{3}}$ approaches almost zero compared with $\pi c / \Lambda$), both the real and imaginary parts of the Bloch wave number K would arise, because the strong dispersion of the EIT medium, of which the relative refractive index is a complex number, plays a key role for creating such a band structure.

In Fig. 5(b) we have shown the fine structure of the band induced by the EIT resonance. However, the detailed fine texture cannot be signified by the coarse curves in Fig. 5(b), since the band structure is plotted within a large range of probe frequency detuning. We shall in what follows treat further the fine structure of the band of EIT-based photonic crystal when the $|1\rangle$ - $|3\rangle$ transition of the EIT atomic levels is on resonance. It follows from Fig. 6(a) that after aligning dielectric GaAs side by side with EIT medium there are three extreme values of imaginary part K'' in the Bloch wave number (or $K'' \rightarrow k_0 n''_{\mathrm{r,(D|E)}}$). Coincidently, there are also three extreme values of real part K' in the Bloch wave number (or $K' \rightarrow k_0 n'_{\mathrm{r,(D|E)}}$). However, neither of them reaches the band edge $K = 0$ or $K = \pm 0.5$ (in the units of $2\pi / \Lambda$). Note that K' and K'' simultaneously exist, since the refractive index of the EIT medium has an imaginary part. It should be emphasized that the band structure (i.e., K' and K'' vary as the probe frequency detuning $\Delta_{\mathbf{p}}$ changes slightly) is very sensitive to the probe frequency detuning. From Fig. 6 (a) one can see that the real part of the Bloch wave number changes drastically from 0 to 0.5 (in the units of $2\pi / \Lambda$) and the imaginary part changes from -0.5 to 0 (in the units of $2\pi / \Lambda$) within a very narrow probe frequency band (namely, a very small change, e.g., at the level of one part in 10^8 in the probe frequency, gives rise to a large variation in the Bloch wave number). In particular, the slope ($\mathrm{d}K / \mathrm{d}\Delta_{\mathrm{p}}$) is almost divergent at the position $\Delta_{\mathbf{p}} / \Gamma_{\mathbf{3}} = 0.5$. The reason for this is because $\Delta_{\mathbf{p}} = 0.5\Gamma_{\mathbf{3}}$ is exactly the two-

photon resonant frequency ($\Delta_p = \Delta_c$). As there is almost divergent dispersion close to $\Delta_p = 0.5\Gamma_3$, the effects of slow light and the negative group velocity in such an EIT-based periodic layered material deserve consideration. This would lead to promising applications in designing devices for slowing down light speed. Besides, the EIT-based band structure is tunable in response to the intensity (characterized by the Rabi frequency Ω_c) of the external control field, since the refractive index of the EIT medium can be controlled by the control field. In Fig. 6 (b) the real part of the Bloch wave number K decreases as Ω_c increases from 0 to $4\Gamma_3$, and then increases when $\Omega_c / \Gamma_3 > 4$; the absolute value of the imaginary part of the Bloch wave number increases first in the range $\Omega_c / \Gamma_3 \in [0,1]$ and then decreases when $\Omega_c / \Gamma_3 > 1$. This, therefore, means that one can use one optical field to controllably manipulate the wave propagation of the other optical field via such an effect of sensitive switching control exhibited in the EIT-based periodic layered structure.

(a)

(b)

(c)

(d)

Fig. 5. The bandgap structure of the 1D infinite periodic (D|E) cells when the probe frequency of TE waves is far from the resonance. In (a) is the band structure in the probe frequency detuning range $\Delta_p / \Gamma_3 \in [-2.5 \times 10^8, +2.5 \times 10^8]$. In (b), (c) and (d) are the fine details exhibited in the EIT-based band structure in the probe frequency detuning ranges (in units of Γ_3), i.e., $\Delta_p / \Gamma_3 \in [-1.7 \times 10^7, +2.0 \times 10^7]$, $[-11.0 \times 10^7, +1.0 \times 10^7]$ and $[-2.5 \times 10^8, 0.0 \times 10^8]$, respectively.

As we have shown the characteristics of both sensitivity and tunability of the EIT-based band structure in Fig. 5(b) and Fig. 6, we shall present its three-dimensional behavior as both the probe frequency detuning and the Rabi frequency of control field vary. The sensitivity and the tunability versus the probe frequency detuning Δ_p and the Rabi frequency Ω_c of control field, respectively, are shown in Fig. 7.

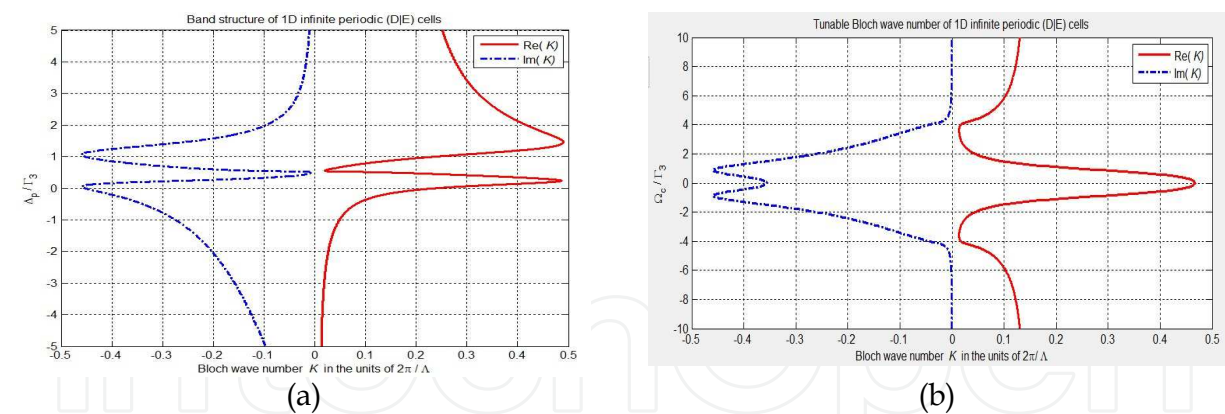(a)   (b)

Fig. 6. The Bloch wave number K of the 1D infinite periodic $(D|E)$ cells when the EIT atomic transition is on resonance. The curves in (a) indicate the real and imaginary parts of the normalized Bloch wave number K sensitive to the probe frequency detuning Δ_p, where the Rabi frequency of the control field is chosen as $\Omega_c = 2.0 \times 10^7$ s^{-1}. The curves in (b) show the tunable Bloch wave number K at the frequency detuning $\Delta_p = 2.0 \times 10^7$ s^{-1} when the Rabi frequency Ω_c of the control field changes.

(a)   (b)

Fig. 7. The real part (a) and the imaginary part (b) of the normalized Bloch wave number K (in the units of $2\pi / \Lambda$) of the 1D infinite periodic $(D|E)$ cells versus Δ_p and Ω_c. Both the real and imaginary parts of the Bloch wave number K are sensitive to the small change in the probe frequency (the slope $dK / d\Delta_p$ of the dispersive curve is much more larger than that in a conventional photonic crystal), and both the real and imaginary parts of the Bloch wave number at any fixed probe frequencies can be controllable by the control Rabi frequency Ω_c.

5. Probe-frequency-sensitive and field-intensity-sensitive coherent control effects in an EIT-based periodic layered medium

We shall now show that the reflection coefficient would be sensitive to the probe frequency when it is tuned onto two-photon resonance ($\Delta_p \to \Delta_c$). The typical atomic and optical parameters for the numerical results are chosen exactly the same as those used in the preceding sections. In Fig. 8, the real and imaginary parts of the reflection coefficient r corresponding to N-layer $(D|E)$ cells are presented as an illustrative example, where the layer number $N = 1, 5, 20, 100$. It can be seen that the reflection coefficient changes

drastically in the frequency detuning range of concern. We plot in Fig. 8 the dispersive behavior of r in the range of $\Delta_p / \Gamma_3 \in [0.3, 0.7]$, i.e., the probe frequency detuning changes at the level of one part in 10^8 in the probe frequency ω_p (the typical value of the probe frequency $\omega_p \simeq 10^{15}$ s^{-1}). It follows from Fig. 8 that the real and imaginary parts of r change from about 0.25 to 0.95 and from about -0.25 to 0.40, respectively. As is expected, such a dramatic change in the coefficient of reflection results from the two-photon resonance (because of the destructive quantum interference between the $|1\rangle$-$|3\rangle$ and $|2\rangle$-$|3\rangle$ transitions). In general, the more layers there are in the dielectric-EIT cell structure, the more drastic change there would be in the reflection coefficient on the left-side interface of this EIT-based periodic layered medium. Thus, the total number of valleys and peaks in the curve of the reflection coefficient r in a narrow band close to $\Delta_p = 0.5\Gamma_3$ becomes more and more as the total layer number N increases. However, such valleys and peaks in the reflection coefficient are no longer conspicuous for the cases of large N, since the amplitudes of fluctuation become smaller when the layer number N is adequately large. If, for example, the layer number $N = 100$, the small fluctuations tend to efface themselves (see Fig. 8).
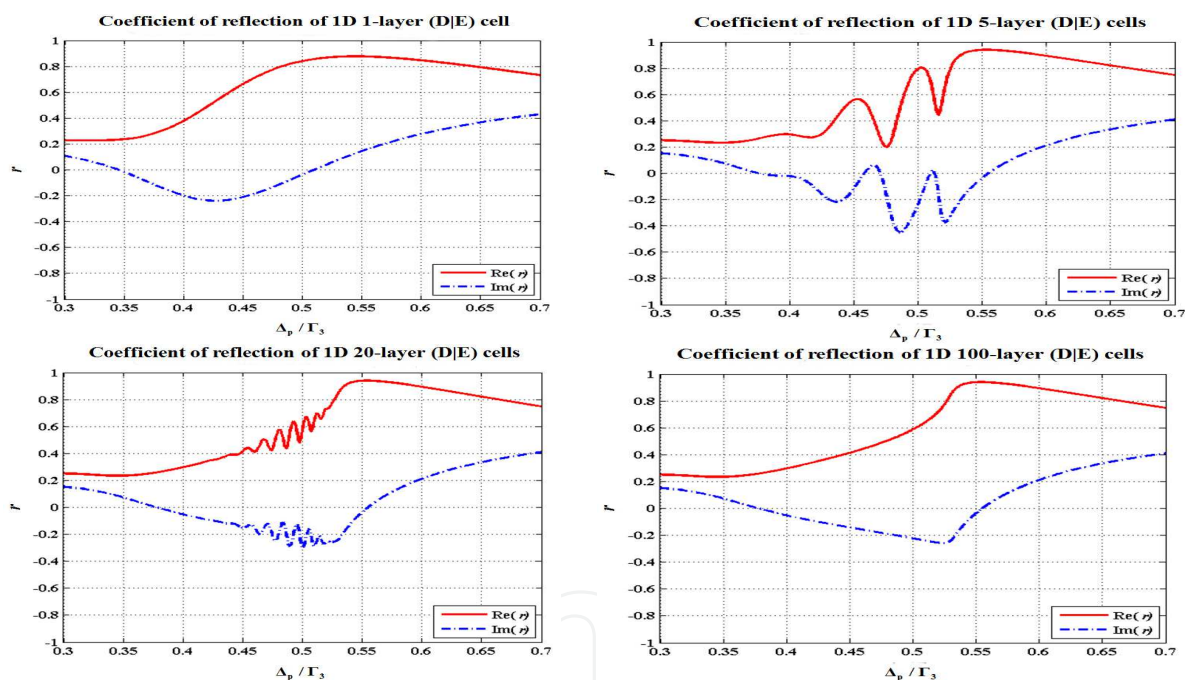

Fig. 8. The real and imaginary parts of the reflection coefficient r versus the normalized probe frequency detuning Δ_p / Γ_3 in the frequency range of two-photon resonance caused by the destructive quantum interference between the $|1\rangle$-$|3\rangle$ and $|2\rangle$-$|3\rangle$ transitions (close to $\Delta_p = 0.5\Gamma_3$). The layer number of the EIT-based periodic medium $N = 1, 5, 20, 100$. The Rabi frequency of the control field is chosen as $\Omega_c = 2.0 \times 10^7$ s^{-1}.

We have demonstrated the probe *frequency-sensitive* behavior of the EIT-based periodic layered material. It can exhibit another effect (field-controlled *tunable* optical response), where the control field can be used to manipulate the photonic band structure, and therefore the reflection coefficient would vary as we tune the control Rabi frequency Ω_c. It follows from Fig. 9 that the tunable reflection coefficient of the EIT-based periodic layered medium

is also sensitive to the Rabi frequency of the control field when the total layer number N increases. This means that the incident probe signal is either reflected or transmitted depending quite sensitively on the intensity of the external control field (characterized by $\Omega_c^* \Omega_c$), and therefore it could be used for designing some sensitive photonic devices (e.g., optical switches, photonic logic gates as well as tunable photonic transistors). In addition, a full controllability of reflection and transmission of the present EIT-based layered structure can also be demonstrated in Fig. 9. It can be readily seen that both the real and imaginary parts of the reflection coefficient r are less than 0.1, and hence the reflectance ($R = r^* r$) approaches zero (or almost zero) when the normalized control Rabi frequency Ω_c / Γ_3 is taken to be certain values, such as $\Omega_c / \Gamma_3 = 6.0$ (for $N = 5$), $\Omega_c / \Gamma_3 = 8.5$ (for $N = 20$) and $\Omega_c / \Gamma_3 = 10, 20$ (for $N = 100$). Thus, a field-intensity-sensitive switchable mirror can be fabricated with the EIT-based layered structure having a large total layer number N (e.g., $N > 100$). The three-dimensional behavior of the reflectance of the EIT-based periodic layered medium as both the Rabi frequency Ω_c and the probe frequency detuning Δ_p change is indicated in Fig. 10. Besides, we also consider the reflectance and transmittance of 1-, 5-, 20-, 100-layer periodic structures at other probe frequency detuning, e.g., $\Delta_p = -10^8$ s^{-1} in Fig. 11 as an illustrative example of tunable field-intensity-sensitive coherent control effect.
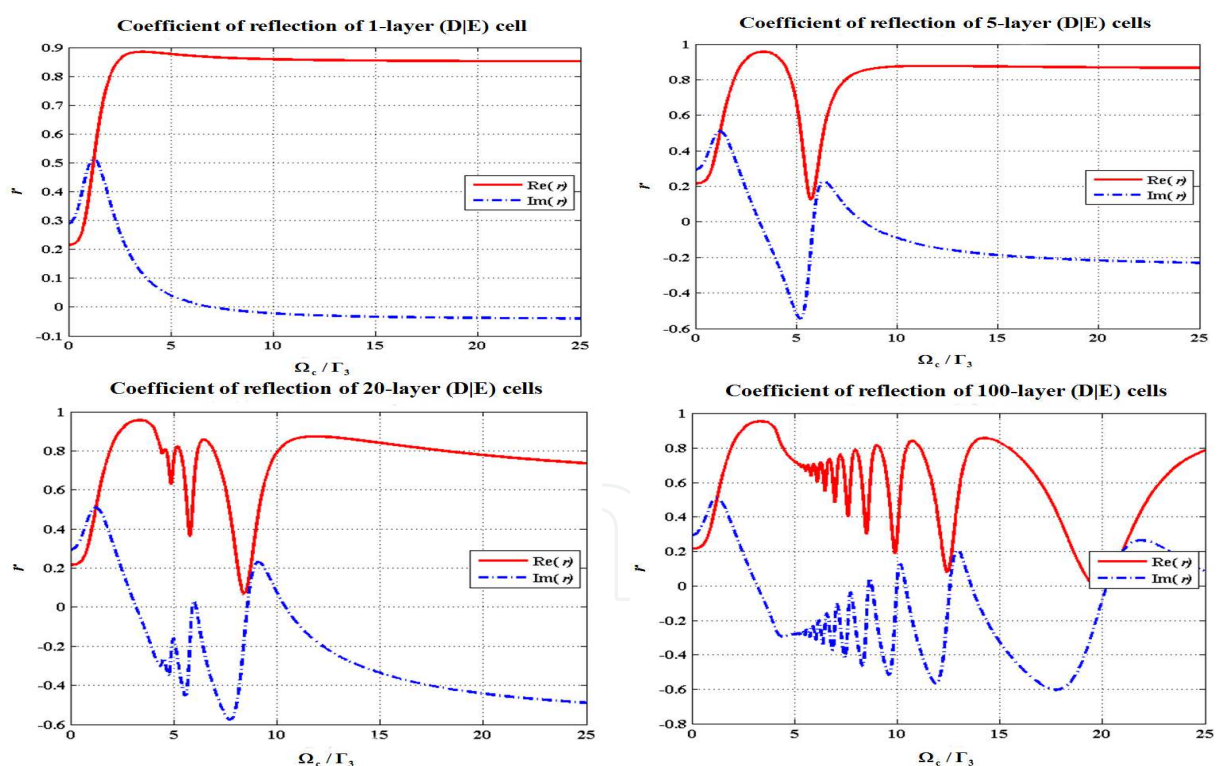

Fig. 9. The real and imaginary parts of the reflection coefficient r versus the normalized Rabi frequency Ω_c / Γ_3 of the control field. The probe frequency detuning is $\Delta_p = 2.0 \times 10^7$ s^{-1}. All the atomic and optical parameters such as $\wp_{31}$, Γ_3, γ_2, Δ_c, N_a are chosen exactly the same as those in Fig. 8. In the case of $N = 100$, the reflection coefficient depends quite sensitively on the Rabi frequency of the control field.
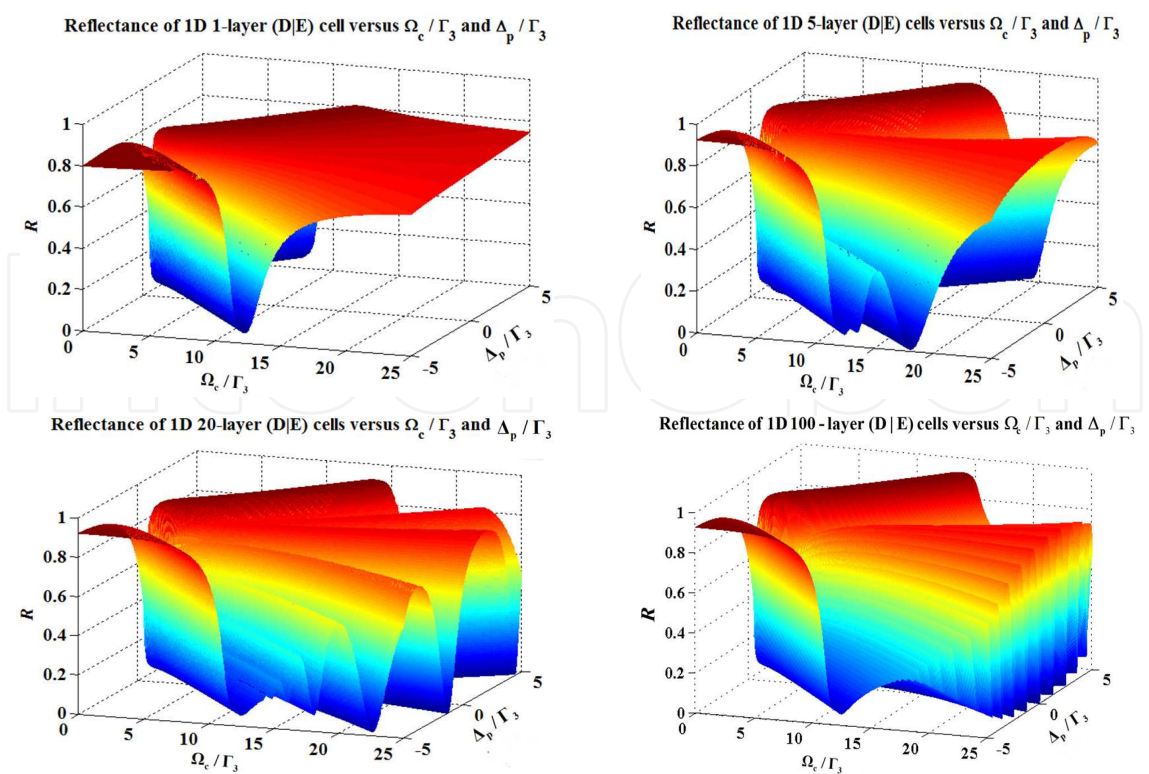
Fig. 10. The three-dimensional behavior of the reflectance of the EIT-based layered medium versus the normalized control Rabi frequency Ω_c / Γ_3 and the normalized probe frequency detuning Δ_p / Γ_3. All the atomic and optical parameters such as $\wp_{31}$, Γ_3, γ_2, Δ_c, and N_a are chosen exactly the same as those in Figs. 8 and 9.

Fig. 11. The reflectance and transmittance versus the normalized Rabi frequency Ω_c / Γ_3 of the control field. The probe frequency detuning is chosen as $\Delta_p = -10^8 \text{ s}^{-1}$. All the atomic and optical parameters such as $\wp_{31}$, Γ_3, γ_2, Δ_c, N_a are chosen exactly the same as those in Fig. 8.

It should be noted that the probe frequency detuning Δ_p does not equal the frequency detuning Δ_c of the control field in Figs. 9-11, which are some typical cases for exhibiting general optical behavior of EIT-based photonic crystals. The quantum interference between atomic transitions (particularly when the condition of two-photon resonance, $\Delta_c = \Delta_p$, is fulfilled) can give rise to a strong dispersion that is tunable by the external control field (characterized by the Rabi frequency Ω_c). The structure of the EIT-based photonic crystal can thus be designed by taking advantage of such an effect of quantum coherence. We expect that the present probe-frequency-sensitive and field-intensity-sensitive coherent control effect with an EIT-based periodic layered structure can be used as a fundamental mechanism for designs and fabrications of new quantum optical and photonic devices.

6. The frequency-sensitive tunable band structure of TM wave

In the preceding two sections we have studied the periodic structure composed of an EIT medium and a normal dielectric (i.e., right-handed material). As a left-handed material (LHM) can exhibit unusual electromagnetic properties (Veselago, 1968), we shall now demonstrate how the layer structure of 1D photonic crystal consisting of the EIT vapor layers and the LHM host dielectric layers can show extraordinary sensitivity to the frequency of the probe field. As the band structure for TM wave seems to be more sensitive to the frequency than that for TE wave (Yeh, 2005), in this section we shall focus our attention on the optical response (e.g., frequency-sensitive band structure induced by two-photon resonance and higher-than-unity reflection coefficients due to the Klein tunneling) of TM wave.

As is well known, the Maxwell curl equations show that the phase velocity of light wave propagating inside a left-handed medium is pointed opposite to the direction of energy flow, that is, the Poynting vector and the wave vector of electromagnetic wave would be anti-parallel (i.e., its wave vector **k**, electric field **E** and magnetic field **H** form a left-handed system). There have been some schemes to achieve the left-handed materials in the literature (Veselago, 1968; Shelby et al., 2001; Pendry et al., 1998; Pendry et al., 1996). Note that a right-handed system can be changed into a left-handed one via the operation of mirror reflection. It is thus clearly seen that the permittivity and the permeability of the free vacuum in a mirror world would be negative numbers. We have therefore pointed out that the electromagnetic wave (or a photon field) propagating inside a left-handed medium behaves like a wave of "antiparticle" of photon (Shen, 2003; Shen, 2008). However, as we know, there exist no such "antiphotons" in nature. The theoretical reason for this is that the four-dimensional electromagnetic vector potentials A_μ with $\mu = 0,1,2,3$ are always taking the real numbers. But in a dispersive and absorptive medium, one can utilize an effective medium theory, where the vector potentials A_μ could probably take complex numbers. Such complex vector field theory has been considered previously (Lurié, 1968). The Lagrangian density of a complex electromagnetic field is given by $\ell = -F_{\mu\nu}^* F^{\mu\nu} / 2$. The complex four-dimensional vector potentials characterize the propagating behavior of both photons and "antiphotons", and hence both the electromagnetic wave characteristics in left- and right-handed media can be treated in a unified framework.

If the light quanta in a medium of negative refractive index can be considered to be the "antiparticles" of photons, it is of interest to propose an optical (or photonic) analog of the well-known Klein paradox, which appears in regimes of relativistic quantum mechanics and

quantum field theory (Calogeracos & Dombey, 1999). In the Klein paradox, the relativistic wave equation can lead to so-called "negative probabilities" induced by certain energy potentials (e.g., the strong repulsive potential barrier with height exceeding the rest energy of particle) (Calogeracos & Dombey, 1999). Such a paradox can be interpreted based on the mechanism of particle-antiparticle pair production, which gives rise to higher-than-unity reflectance and negative transmittance. The Klein tunneling has been expected to be observed in QED regime, where an incoming electron wave function propagates and penetrates through a sufficiently high potential barrier. Though such a counterintuitive effect of relativistic quantum tunneling can be explained by using the notion of creation of electron-positron pairs, which is a physical process at the potential discontinuity, even today it is still referred to as "Klein paradox" in order to indicate its anomalous tunneling characteristics. Since the electron is massive, it is in fact quite difficult to realize the exotic Klein tunneling experimentally. Here, we shall suggest an alternative way to realize this intriguing effect, i.e., the photonic analog of Klein tunneling in an LHM-EIT-based periodic layered medium, where the reflection coefficient exceeding unity will also occurs in some frequency ranges, and this will lead to a negative transmittance.

The 1D periodic LHM-EIT cells are embedded in a left-handed homogeneous dielectric (an LHM-EIT cell consists of a left-handed dielectric and an EIT atomic medium). Fig. 12 indicates the band structure of the 1D infinite periodic LHM-EIT cells (sketched in Fig. 4) when the TM wave of the probe beam whose magnetic field vector is perpendicular to the x-z plane (Yeh, 2005) is incident normally or obliquely on such a periodic layered medium. Here we also choose the typical atomic ($|1\rangle$ - $|3\rangle$) transition frequency $\omega_{31} = 5.0 \times 10^{15}$ s^{-1}, and the thickness of the two layers $a = 0.1\mu$m (left-handed dielectric) and $b = 0.1\mu$m (EIT medium). The thickness of one LHM-EIT cell is $\Lambda = a + b$. We plot in Fig. 12 the dispersive behavior of six typical cases (i.e., the angles of incidence θ_i are $0^o, 15^o, 30^o, 45^o, 60^o$, and 75°, respectively). The tunable Rabi frequency Ω_c of the control field chosen for the present scheme is 2.0×10^7 s^{-1}.
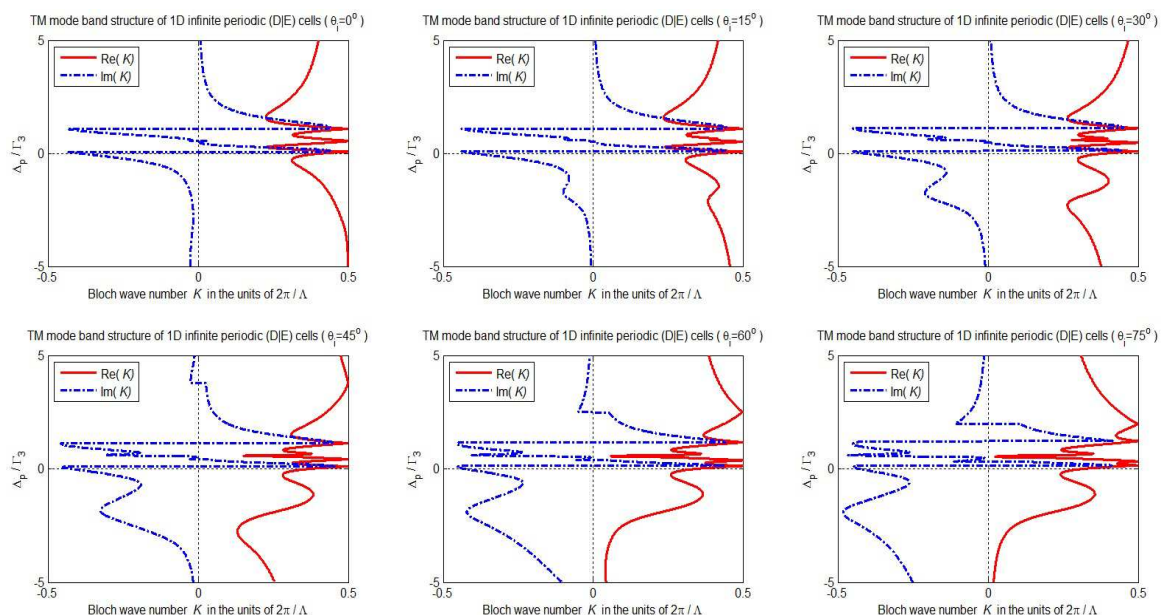

Fig. 12. The band structure of the 1D infinite periodic LHM-EIT cells when the angles of incidence of the TM wave of the probe beam are $\theta_i = 0^o, 15^o, 30^o, 45^o, 60^o, 75^o$, respectively.

As the refractive index of the EIT medium has an imaginary part in the frequency range of concern (see Fig. 12), the real part $\text{Re}(K)$ and the imaginary part $\text{Im}(K)$ of the Bloch wave number simultaneously exist. We emphasize that the band structure (i.e., K vary dramatically as the probe frequency detuning Δ_p changes slightly) is very sensitive to the probe frequency detuning. It follows that in a very narrow frequency band, where Δ_p is close to the resonance position, namely, the EIT two-photon resonance occurs ($\Delta_p \to \Delta_c$, i.e., $\Delta_p / \Gamma_3 \to 0.5$), both the real and imaginary parts of the Bloch wave number change drastically in a wide range, e.g., [0, 0.5] (in the units of $2\pi / \Lambda$) for $\text{Re}(K)$ and [-0.5, $+0.5$] for $\text{Im}(K)$. Since the EIT two-photon resonance arises at $\Delta_p = \Delta_c$ with the control frequency detuning $\Delta_c = 1.0 \times 10^7 \text{ s}^{-1}$, and the probe transition frequency $\omega_{31} = 5.0 \times 10^{15} \text{ s}^{-1}$, a very small change (e.g., at the level of one part in 10^8) in the probe frequency would result in a large variation in the Bloch wave number. For this reason, the slope ($dK / d\Delta_p$) of the Bloch dispersive curves is almost divergent at the position $\Delta_p / \Gamma_3 = 0.5$. Since there is strong dispersion in the curves of Bloch wave number K in the vicinity of $\Delta_p = 0.5\Gamma_3$, the effects of slow light as well as the negative group velocity would arise in the present periodic layered material.
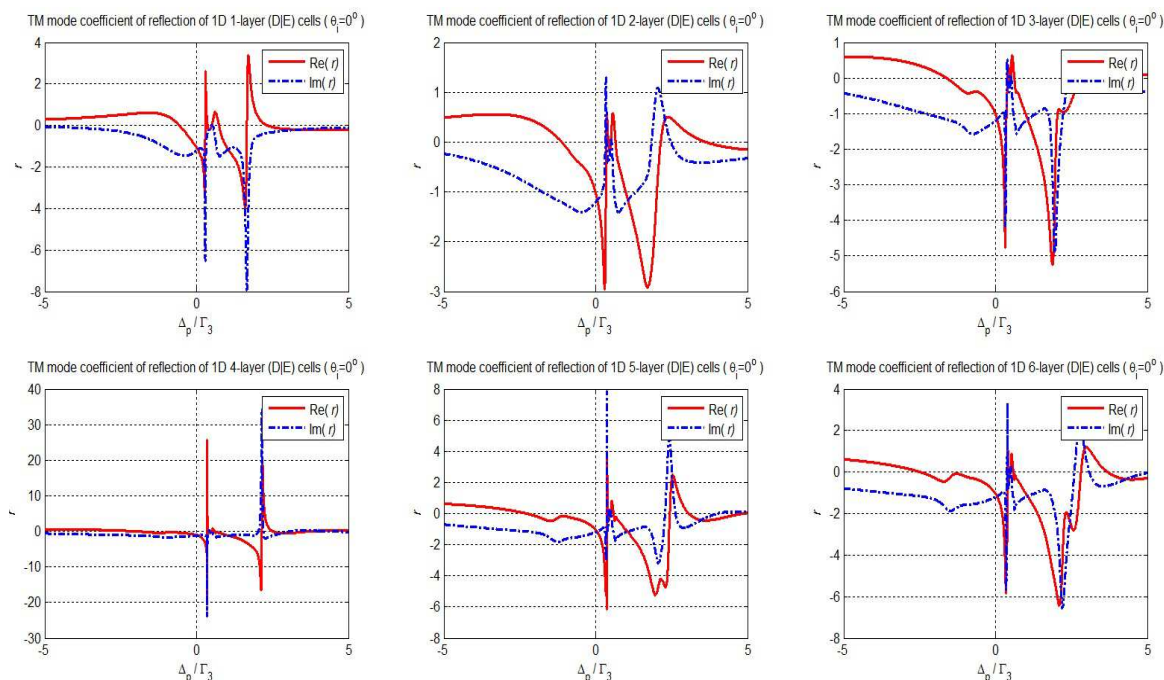

Fig. 13. The real and imaginary parts of the reflection coefficient r corresponding to the N-layer LHM-EIT cells ($N = 1 - 6$), where the relative refractive index of the left-handed medium is $n_1 = -1$. The photonic Klein tunneling occurs, i.e., in some frequency ranges the absolute values of both the real and imaginary parts of the reflection coefficient r are larger than unity.

We are now in a position to address the problem of reflection and transmission of the present photonic crystal. Obviously, the reflectance and transmittance would also be sensitive to the probe frequency when it is tuned onto resonance ($\Delta_p \to \Delta_c$). In Fig. 13 the real and imaginary parts of the reflection coefficient r corresponding to the N-layer LHM-EIT cells are presented as an illustrative example, where the layer number $N = 1 - 6$ and the Rabi frequency of the control field is chosen as $\Omega_c = 2.0 \times 10^7 \text{ s}^{-1}$. The TM wave is incident

normally on the periodic layered structure. It can be seen that both the real and imaginary parts of the reflection coefficient r in all the cases (i.e., the layer number $N = 1 - 6$) change drastically as the probe frequency is close to the resonant frequency (at $\Delta_p = 0.5\Gamma_3$, where the probe frequency is tuned onto the two-photon resonance of the EIT atomic system).

As the layered medium contains the left-handed layers, and the periodic EIT layers act as a potential barrier for the incident electromagnetic wave, the absolute values of the real or imaginary part of the reflection coefficient r in some frequency ranges is larger than unity because of the Klein tunneling. In order to show the exotic and counterintuitive features exhibited in Fig. 13, we will present the behavior of reflection of TM wave by a RHM-EIT-based periodic layered structure, in which the left-handed layers have been replaced with the right-handed medium (or vacuum), for comparison. In the reflection coefficient of the N-layer RHM-EIT cells, in which the relative refractive index of the right-handed medium is $n_1 = +1$, is shown in Fig. 14. In this case, both the host dielectric layers and the EIT layers are right-handed media, so that there is no Klein tunneling, i.e., the absolute values of both the real and imaginary parts of the reflection coefficient r are less than unity. This, therefore, means that the left-handed dielectric is requisite in order to achieve the unusual photonic tunneling in the periodic layer structure containing EIT medium.
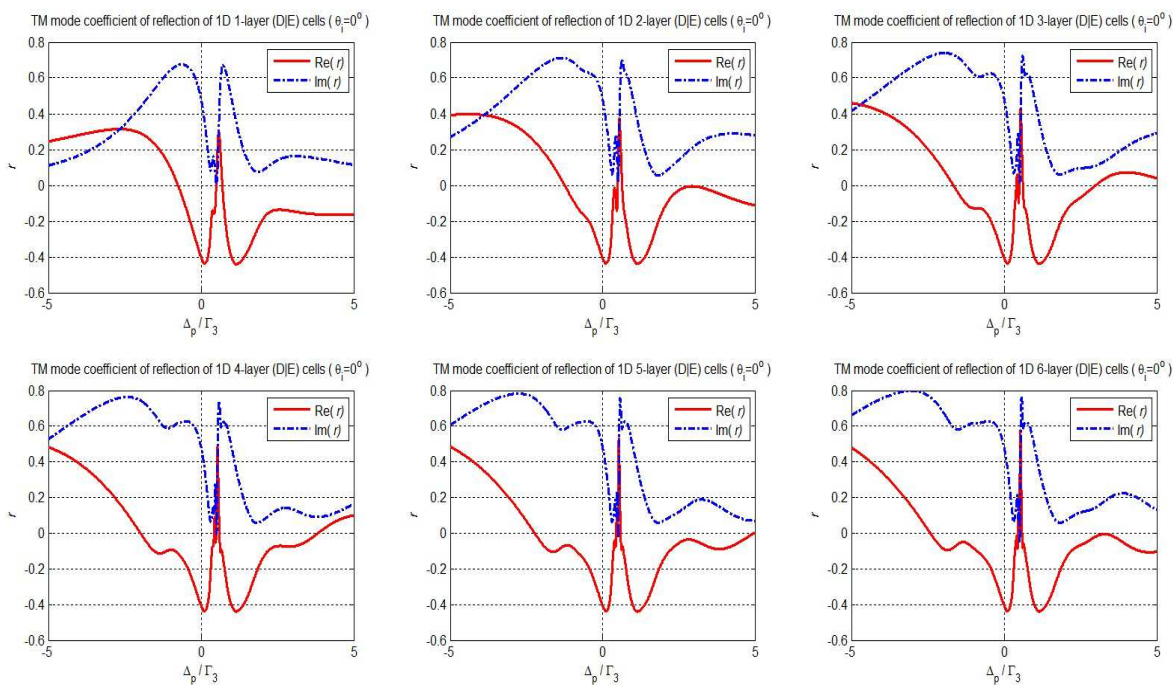

Fig. 14. The real and imaginary parts of the reflection coefficient r corresponding to the N-layer LHM-EIT cells ($N = 1 - 6$), where the relative refractive index of the right-handed medium is $n_1 = +1$. There is no photonic Klein tunneling, i.e., the absolute values of both the real and imaginary parts of the reflection coefficient r are less than unity.

7. A potential application: Photonic transistors and logic gates

We have shown that the LHM-EIT-based periodic medium can give rise to extraordinary reflection and transmission. Now we shall consider the physical meanings of such a photonic analog of Klein tunneling as well as its photonic application to device design.

The reflectance R and transmittance T on the left interface of the LHM-EIT structures are given in Figs. 15 and 16 as an illustrative example. It follows that the reflectance (and transmittance) is quite sensitive to the probe frequency detuning in some frequency ranges. It seems that the reflected wave intensity is larger than the incident intensity. This is because the additional particles are supplied by the potential barrier (Klein tunneling). Correspondingly, the transmitted wave is opposite in the intensity to the incident wave. In this process, the conservation of both the energy and the photon number is guaranteed. For example, the current density of the complex electromagnetic field can be defined as $J_\nu = \mathrm{i}(A_\mu F_\nu{}^{\mu*} - A_\mu^* F_\nu{}^\mu)$ whose four-dimensional divergence is given by

$$\partial^\nu J_\nu = \mathrm{i}\partial^\nu(A_\mu F_\nu{}^{\mu*} - A_\mu^* F_\nu{}^\mu) = \mathrm{i}(\partial^\nu A_\mu)F_\nu{}^{\mu*} - \mathrm{i}(\partial^\nu A_\mu^*)F_\nu{}^\mu \cdot \qquad (14)$$

The above equation can be rewritten as $\mathrm{i}(F^\nu{}_\mu + \partial_\mu A^\nu)F_\nu{}^{\mu*} - \mathrm{i}(F^{\nu*}{}_\mu + \partial_\mu A^{\nu*})F_\nu{}^\mu$ $= \mathrm{i}(\partial_\mu A^\nu)F_\nu{}^{\mu*} - \mathrm{i}(\partial_\mu A^{\nu*})F_\nu{}^\mu$, where the electromagnetic field equations $\partial_\mu F_\nu{}^{\mu*} = 0$, $\partial_\mu F_\nu{}^\mu = 0$ have been employed. With the help of the electromagnetic field equations, one can arrive at $\partial^\nu J_\nu = \mathrm{i}\partial_\mu(A^\nu F_\nu{}^{\mu*} - A^{\nu*} F_\nu{}^\mu)$. Thus, the four-dimensional divergence of current density is

$$\partial^\nu J_\nu = \mathrm{i}\partial_\upsilon(A^\mu F_\mu{}^{\nu*} - A^{\mu*} F_\mu{}^\nu) \cdot \qquad (15)$$

It follows from Eqs. (14) and (15) that $\partial^\nu J_\nu = 0$ (this means that the current density of the complex electromagnetic field obeys the law of conservation). If the Hermitian field operator A_μ can be written as

$$A_\mu \sim \int \mathrm{d}^3 k \left[a_{(\lambda)}(\mathbf{k},t)\mathrm{e}^{\mathrm{i}k\cdot x} + b_{(\lambda)}^+(\mathbf{k},t)\mathrm{e}^{-\mathrm{i}k\cdot x} \right] e_\mu^{(\lambda)},$$
$$A_\mu^+ \sim \int \mathrm{d}^3 k \left[a_{(\lambda)}^+(\mathbf{k},t)\mathrm{e}^{-\mathrm{i}k\cdot x} + b_{(\lambda)}(\mathbf{k},t)\mathrm{e}^{\mathrm{i}k\cdot x} \right] e_\mu^{(\lambda)}, \qquad (16)$$

where $e_\mu^{(\lambda)}$ denotes the polarization vector, the "Noether charge" corresponding to the current density J_ν of the complex electromagnetic field is given by

$$\int \mathrm{d}^3 x J_0 \sim \int \mathrm{d}^3 k \sum_{\lambda=0}^{3} \left[a_{(\lambda)}^+(\mathbf{k},t)a_{(\lambda)}(\mathbf{k},t) - b_{(\lambda)}^+(\mathbf{k},t)b_{(\lambda)}(\mathbf{k},t) \right]. \qquad (17)$$

Here, $a_{(\lambda)}(\mathbf{k},t)$, $a_{(\lambda)}^+(\mathbf{k},t)$, $b_{(\lambda)}(\mathbf{k},t)$, $b_{(\lambda)}^+(\mathbf{k},t)$ stand for the annihilation and creation operators of photons and its "antiparticles", respectively. The term $a_{(\lambda)}^+(\mathbf{k},t)a_{(\lambda)}(\mathbf{k},t)$ in Eq. (17) is the total number of photons, while $-b_{(\lambda)}^+(\mathbf{k},t)b_{(\lambda)}(\mathbf{k},t)$ is the total number of the "antiparticle" of photon. It can be seen that the total number of the "antiparticle" is negative.

The photonic analog of the Klein tunneling presented here can be used to design the so-called frequency-sensitive photonic transistors (see Fig. 17(a) for a schematic diagram) that can switch the photonic signals: specifically, the incident probe beam, the reflected probe beam, and the transmitted probe beam can mimic the operation of the three terminals (i.e., base, collector and emitter, respectively) of a bipolar transistor (a semiconductor device for amplifying and switching electronic signals). A small intensity of probe beam at the base terminal can manipulate (or switch) a much larger intensity between the terminals of collector (reflected probe beam) and the emitter (transmitted probe beam), since the incident probe beam can control the reflected wave in proportion to the input signal (incident probe beam).
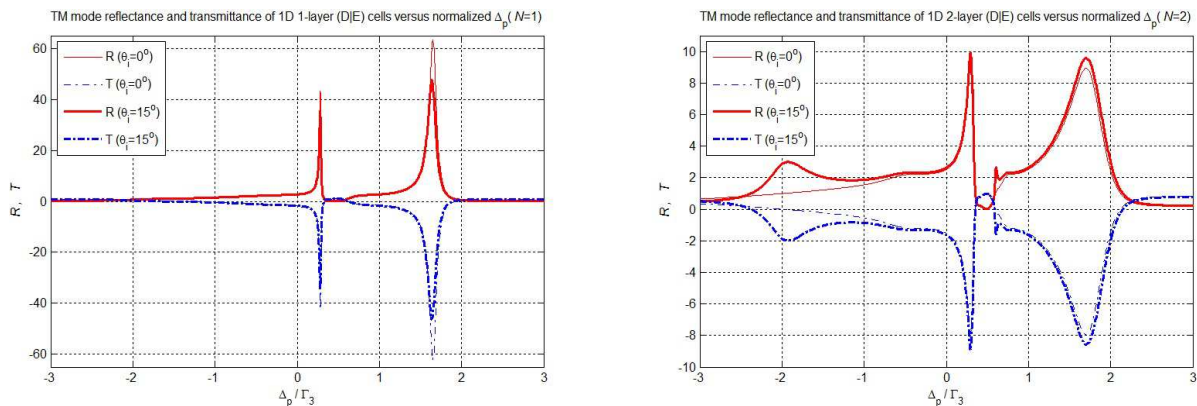
Fig. 15. The reflectance and transmittance of 1-layer and 2-layer LHM-EIT structures (the relative refractive index of the left-handed medium $n_1 = -1$) in the probe frequency range $\Delta_p / \Gamma_3 \in [-3, 3]$.
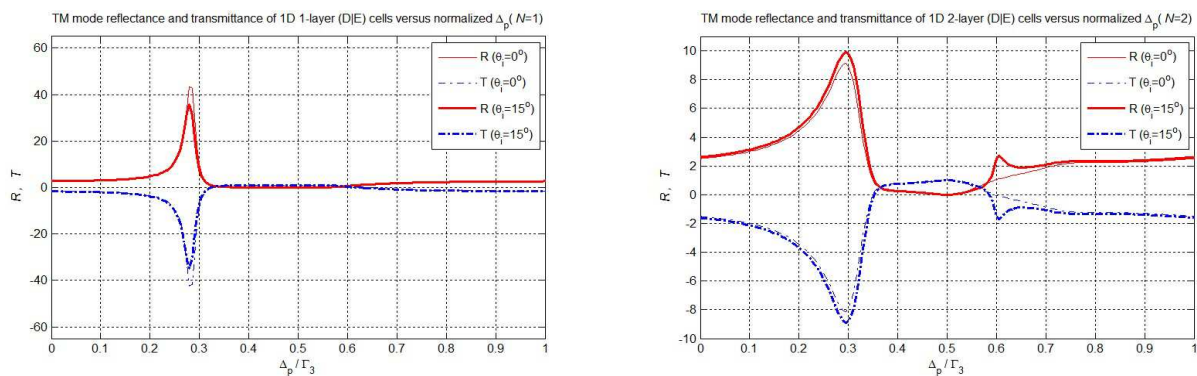

Fig. 16. The reflectance and transmittance of 1-layer and 2-layer LHM-EIT structures (the relative refractive index of the left-handed medium $n_1 = -1$) in the probe frequency range $\Delta_p / \Gamma_3 \in [0, 1]$.

As we have pointed out in the preceding sections, the sensitive optical switching control can also be utilized to design photonic logic gates by means of such an EIT-based periodic layered structure. For example, the incident probe beam and the applied control field can act as the two input signals. We suppose that the output signal $Y = 1$ if the probe field can propagate through the periodic layered medium, and the output signal $Y = 0$ if the probe beams cannot be transmitted through the structure (i.e., the reflection and absorption dominates in the probe wave propagation). Then the logic operations of two-input AND gate can be implemented with such a layered structure. Alternatively, we can also apply at least two probe waves at different wavelengths, which correspond to different transmittances. In this new scenario, the two incident probe beams of different frequencies can stand for the two input signals (see Figs. 17 and 18). Therefore, the functional and logic gates, such as NAND, NOR, EXOR and EXNOR gates, can be designed by taking advantage of the effect of sensitive control for optical switching (due to two-photon resonance of EIT) exhibited in such an EIT-based periodic layered medium.
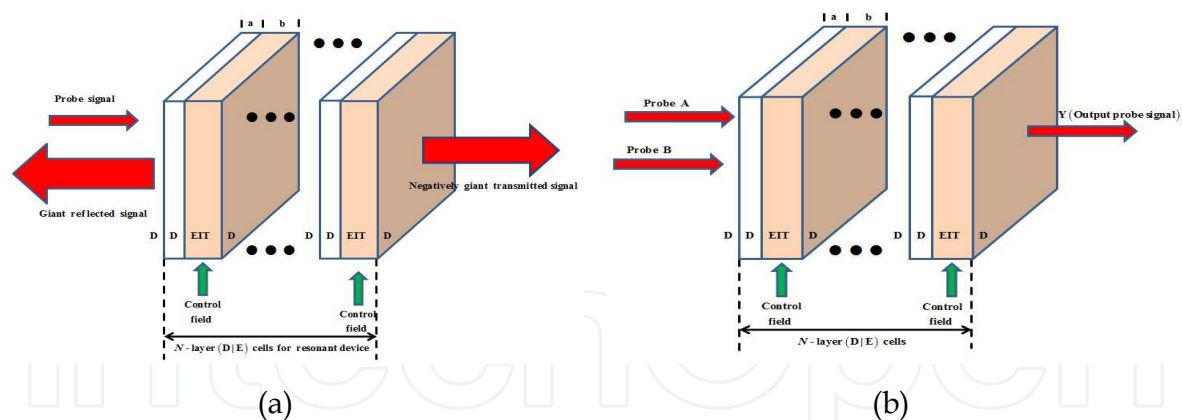
Fig. 17. (a) The schematic diagram of a photonic transistor designed based on the LHM-EIT layered structure. The probe field is incident on the structure, and the giant reflected wave with higher-than-unity reflectance and the transmitted wave with negative transmittance will be produced via the intriguing Klein tunneling effect. The incident probe wave, the reflected wave, and the transmitted wave correspond to the terminals of base, collector and emitter, respectively.

(b) The schematic diagram of a two-input photonic logic gate designed based on the EIT-based layered structure. The two incident probe beams at different frequencies represent the two input signals.

8. Design of two-input photonic logic gates

The dramatic reduction and enhancement in the reflectance and transmittance close to $\Delta_p = 0.5\Gamma_3$ is of special interest since the two-photon resonance ($\Delta_p = \Delta_c$) can give rise to the effect of sensitive optical switching control, which would lead to promising applications to new photonic device design. We shall suggest the working mechanism of two photonic logic gates (e.g., OR and NAND gates), which can be fabricated based on such an EIT-based periodic structure. The fine structure of the reflectance and transmittance for showing extraordinary sensitivity to the frequency of the probe field is demonstrated in Fig. 19(a). Here we plot only the reflectance and transmittance of two cases ($N = 4$ and $N = 6$) as an illustrative example. It can be seen that some oscillations in the curves are exhibited in the narrow resonant frequency range $\Delta_p \in [0.2\Gamma_3, 0.7\Gamma_3]$.

One can see from Fig. 18 (a) that there is a minimum (i.e., 0.19) and a maximum (i.e., 0.99) in the transmittance T at $\Delta_p = 0.53\Gamma_3$ and $0.46\Gamma_3$, respectively, for the 6-layer periodic structure. For the 4-layer periodic structure, however, the transmittance T has a maximum (i.e., 0.99) and a minimum (i.e., 0.34) close to $\Delta_p = 0.53\Gamma_3$ and $0.46\Gamma_3$, respectively. Two structures of layer number $N = 4$ and 6 are sketched in Fig. 18(b). Two probe beams with $\Delta_p = 0.46\Gamma_3$ and $0.53\Gamma_3$, which can act as the two input signals, are applied. We suppose that the output signal $Y = 0$ if neither of the two incident probe beams propagates through the periodic layered medium (i.e., the reflection dominates in the wave propagation of the probe field), and the output signal $Y = 1$ if at least one of the probe beams can be transmitted through the structure (i.e., the reflection and absorption can be ignored). Let the probe beams of $\Delta_p = 0.46\Gamma_3$ and $0.53\Gamma_3$ represent the input signals 0 and 1, respectively. Then the logic operations of two-input OR gate and NAND gate can be implemented with the 4-layer and 6-layer structures, respectively. The truth table of the OR and NAND gates are given as follows:

IN_A	IN_B	$Y = A + B$ (4-layer OR gate)	$Y = \overline{A \cdot B}$ (6-layer NAND gate)
0 $(0.46\Gamma_3)$	0 $(0.46\Gamma_3)$	0	1
0 $(0.46\Gamma_3)$	1 $(0.53\Gamma_3)$	1	1
1 $(0.53\Gamma_3)$	0 $(0.46\Gamma_3)$	1	1
1 $(0.53\Gamma_3)$	1 $(0.53\Gamma_3)$	1	0

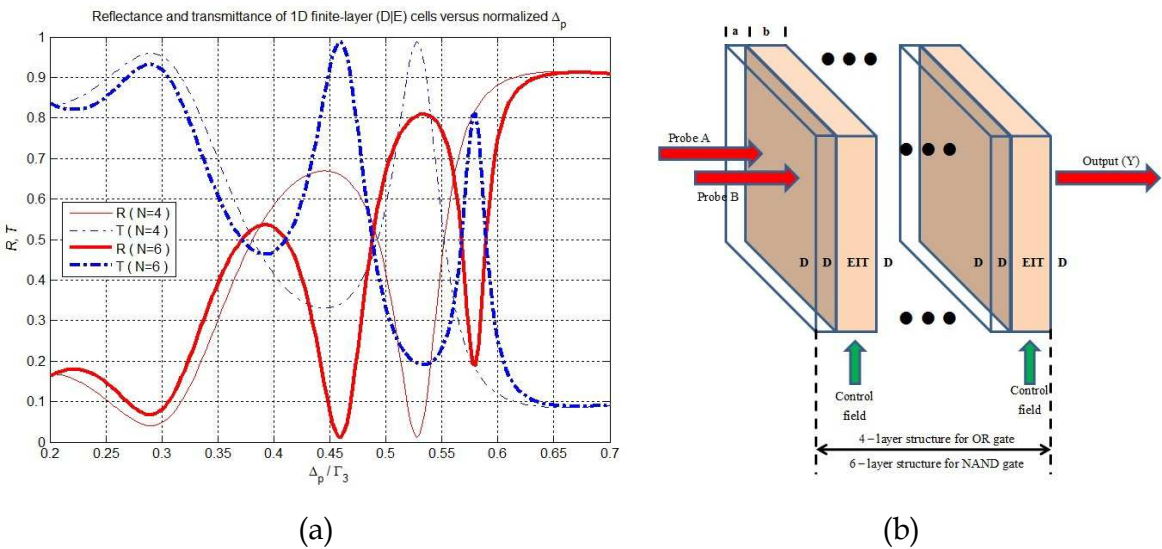Table 1. The truth table of two-input OR gate (fabricated based on the 4-layer periodic structure) and two-input NAND gate (fabricated based on the 6-layer periodic structure).

(a)   (b)

Fig. 18. The fine structure of the reflectance and transmittance of the 4-layer and 6-layer periodic (D|E) cells in a narrow probe frequency band (a), and the schematic diagram of photonic logic gates (b). The Rabi frequency of the control field is $\Omega_c = 4.0 \times 10^7$ s^{-1}.

9. Conclusions

The quantum optical properties of an EIT medium has been discussed (in Section 2), and the formalism for treating wave propagation in a periodic structure has been reviewed (in Section 3). The band structure and the reflectance of a 1D photonic crystal consisting of both EIT medium layers and host dielectric layers can show extraordinary sensitivity to the frequency of a probe field because of a two-photon resonance relevant to destructive quantum interference between two transition pathways driven by the control and probe fields (in Sections 4 and 5). Such an EIT-based periodic layered material can also exhibit an effect of field-intensity-sensitive switching control (depending quite sensitively on the Rabi frequency of the control field) in the cases of large layer number N. Since the optical responses can be controlled by the tunable quantum interference induced by the external control field via two-photon resonance, the EIT-based layered medium under consideration shows more flexible optical responses than conventional photonic crystals because of the EIT two-photon resonance that gives rise to strong dispersion in the band of transparency window.

As the microscopic electric polarizability as well as the electric permittivity of the EIT medium are caused by the atomic energy level transition processes from the ground state to the excited states, in which the quantum interference relevant to atomic phase coherence is involved, the reflectance and transmittance of an EIT-based periodic layered medium are shown to be quite sensitive to the probe frequency.

The LHM-EIT-based periodic layered medium has also been considered (in Sections 6 and 7). Since there are left-handed layers embedded in the layered medium, and the periodic EIT layers would act as a potential barrier for the incident electromagnetic wave, the absolute values of the real or imaginary part of the reflection coefficient in some frequency ranges would be more than unity due to the Klein tunneling. The present photonic analog of the Klein tunneling might be used for designing frequency-sensitive photonic transistors. We expect that some new photonic devices (e.g., logic and functional gates) and sensitively switchable devices (fundamental building blocks in, e.g., photonic microcircuits on silicon, in which light replaces electrons), which would find new applications in photonic quantum information processing, would be achieved by taking advantage of such an effect of *coherent switching control* (in Section 8).

The present scheme can be generalized to the cases of four-level EIT systems, where two control fields and one probe field drive the atomic level transitions (Shen, 2007; Shen & Zhang, 2007; Gharibi et al., 2009; Shen, 2010). Obviously, the optical response in such a four-level EIT-based photonic crystal would be more sensitive to the probe frequency than in a three-level EIT photonic crystal presented in this paper. Apart from this intriguing property, there are also interesting applications based on the four-level EIT photonic crystal, e.g., some examples of photonic devices (e.g., multi-input logic gates), in which the control fields and the transmitted probe field act as the input and output signals, respectively, can be designed. We expect that all these new optical properties relevant to quantum coherence, including their applications to photonic devices, could be realized experimentally in the near future.
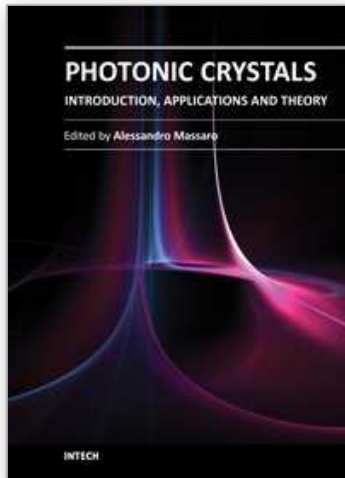
10. Acknowledgments

11. References

Abdumalikov, A. A.; Astafiev, Jr., O.; Zagoskin, A. M.; Pashkin, Y. A.; Nakamura, Y. & Tsai, J. S. (2010). Solitons in Weakly Nonlocal Media with Cubic-Quintic Nonlinearity. *Physical Review Letters,* Vol 104, 193601(1-4), ISSN 0031-9007

Arve, P.; Jänes, P. & Thylén, L. (2004). Propagation of Two-Ddimensional Pulses in Electromagnetically Induced Transparency Media. *Physical Review A,* Vol 69, 063809(1-8), ISSN 1050-2947

Calogeracos, A. & Dombey, N. (1999). History and Physics of the Klein Paradox. *Contemporary Physics,* Vol 40, No. 5, pp. 313–321, ISSN 0010-7514

Caloz, C. & Itoh, T. (2006). *Electromagnetic Metamaterials: Transmission Line Theory and Microwave Applications,* Chapt. 2, John Wiley & Sons, Inc., ISBN 978-047-1669-85-2, New Jersey, USA

Champenois, C.; Morigi, G. & Eschner, J. (2006). Quantum Coherence and Population Trapping in Three-Photon Processes. *Physical Review A,* Vol 74, 053404(1-10), ISSN 1050-2947

Cohen, J. L. & Berman, P. R. (1997). Amplification without Inversion: Understanding Probability Amplitudes, Quantum Interference, and Feynman Rules in a Strongly Driven System. *Physical Review A*, Vol 55, pp. 3900-3917, ISSN 1050-2947

Forsberg, E. & She, J. (2006). Tunable Photonic Crystals Based on EIT Media. *Optoelectronic Materials and Devices* (edited by Lee, Y. H., Koyama, F. & Luo, Y.), *Proc. of SPIE.* Vol 6352, 63520S, ISSN 0277-786X

Gandman, A.; Chuntonov, L.; Rybak, L. & Amitay, Z. (2007). Coherent Phase Control of Resonance-Mediated (2+1) Three-Photon Absorption. *Physical Review A,* Vol 75, 031401(1-4), ISSN 1050-2947

Gharibi, A.; Shen, J. Q. & Gu, J. (2009). Tunable Transient Evolutional Behaviors of a Four-Level Atomic Vapor and the Application to Photonic Logic Gates. *Journal of Physics B: Atomic, Molecular and Optical Physics,* Vol 42, 055502(1-8), ISSN 0953-4075

Harris, S. E. (1997). Electromagnetically Induced Transparency. *Physics Today,* Vol 50, No.7, pp. 36-42, ISSN 0031-9228

He, Q.-Y.; Wu, J.-H.; Wang, T.-J. & Gao, J.-Y. (2006). Dynamic Control of the Photonic Stop Bands Formed by a Standing Wave in Inhomogeneous Broadening Solids. *Physical Review A,* Vol 73, 053813(1-6), ISSN 1050-2947

Joannopoulos, J. D.; Mead, R. D. & Winn, J. N. (1995). *Photonic Crystals: Molding the Flow of Light,* Princeton University Press, ISBN 978-069-1124-56-8, Princeton, New Jersey, USA

Joannopoulos, J. D.; Villenenve, P. & Fan, S. (1997). Photonic Crystals: Putting a new Twist on Light. *Nature,* Vol 386, pp. 143-149, ISSN 0028-0836

Kawazoe, T.; Kobayashi, K.; Sangu, S. & Ohtsu, M. (2003). Demonstration of a Nanophotonic Switching Operation by Optical Near-Field Energy Transfer. *Applied Physics Letters,* Vol 82, pp. 2957-2959, ISSN 0003-6951

Krowne, C. M. & Shen, J. Q. (2009). Dressed-State Mixed-Parity Transitions for Realizing Negative Refractive Index. *Physical Review A,* Vol 79, 023818 (1-11), ISSN 1050-2947

Lurié, D. (1968). *Particles and Fields,* Chapt. 2, Wiley, ISBN 978-047-0556-42-9, New York, USA

Pendry, J. B.; Holden, A. J.; Robbins, D. J. & Stewart, W. J. (1998). Low Frequency Plasmons in Thin Wire Structures. *Journal of Physics: Condensed Matter,* Vol 10, pp. 4785-4809, ISSN 0953-8984

Pendry, J. B.; Holden, A. J.; Stewart, W. J. & Youngs, I. (1996). Extremely Low Frequency Plasmons in Metallic Mesostructures. *Physical Review Letters,* Vol 76, pp. 4773-4776, ISSN 0031-9007

Petrosyan, D. Tunable Photonic Band Gaps with Coherently Driven Atoms in Optical Lattices. *Physical Review A,* Vol 76, (2007), 053823(1-10), ISSN 1050-2947

Sangu, S.; Kobayashi, K.; Shojiguchi, A. & Ohtsu, M. (2004). Logic and Functional Operations Using a Near-Field Optically Coupled Quantum-Dot System. *Physical Review B,* Vol 69, 115334(1-13), ISSN 0163-1829

Schmidt, H. & Imamoğlu, A. (1996). Giant Kerr Nonlinearities Obtained by Electromagnetically Induced Transparency. *Optics Letters,* Vol 21, pp. 1936-1938, ISSN 0146-9592

Scully, M. O. & Zubairy, M. S. (1997). *Quantum Optics,* Chapt. 7, Cambridge Univ. Press, ISBN 0521435951, Cambridge, UK

Shelby, R. A.; Smith, D. R. & Schultz, S. (2001). Experimental Verification of a Negative Index of Refraction. *Science,* Vol 292, pp. 77-79, ISSN 1095-9203

Shen, J. Q. & Zhang, P. (2007). Double-Control Quantum Interferences in a Four-Level Atomic System. *Optics Express,* Vol 15, pp. 6484-6493, ISSN 1094-4087

Shen, J. Q. (2003). Anti-Shielding Effect and Negative Temperature in Instantaneously Reversed Electric Fields and Left-Handed Media. *Physica Script,* Vol 68, pp. 87-97, ISSN 0031-8949

Shen, J. Q. (2007). Transient Evolutional Behaviours of Double-Control Electromagnetically Induced Transparency. *New Journal of Physics,* Vol 15, pp. 374-388, ISSN 1367-2630

Shen, J. Q. (2008). *Classical & Quantum Optical Properties of Artificial Electromagnetic Media,* Chapt. 1, pp. 15-16, Transworld Research Network, ISBN 978-817-8953-56-4, Kerala, India

Shen, J. Q. (2010). Coherence Control for Photonic Logic Gates via Y-Configuration Double-Control Quantum Interferences. *Optics Communications,* Vol 283, pp. 4546–4550, ISSN 0030-4018

Shen, J. Q.; Ruan, Z. C. & He, S. (2004). Influence of the Signal Light on the Transient Optical Properties of a Four-Level EIT Medium. *Physics Letters A,* Vol 330, pp. 487-495, ISSN 0375-9601

Veselago, V. G. (1968). The Electrodynamics of Substances with Simultaneously Negative Values of ε and μ. *Soviet Physics Uspekhi,* Vol 10, pp. 509-514, ISSN 0038-5670

Wang, L. J.; Kuzmich, A. & Dogariu, A. (2000). Gain-Assisted Superluminal Llight Propagation. *Nature,* Vol 406, pp. 277-279, ISSN 0028-0836

Wu, J. H.; Wei, X. G.;, Wang D. F.; Chen, Y. & Gao, J. Y. (2004). Coherent Hole-Burning Phenomenon in a Doppler Bbroadened Three-Level Lambda-Type Atomic System. *Journal of Optics B: Quantum and Semiclassical Optics,* Vol 6, pp. 54-58, ISSN 1464-4266

Yablonovitch, E. (1987). Inhibited Spontaneous Emission in Solid-State Physics and Electronics. *Physical Review Letters,* Vol 58, pp. 2059-2062, ISSN 0031-9007; John, S. (1987). Strong Localization of Photons in Certain Disordered Dielectric Superlattices. *Physical Review Letters,* Vol 58, pp. 2486-2489, ISSN 0031-9007

Yeh, P. (2005). *Optical Waves in Layered Media,* Chapts. 4-6, pp. 83-143, John Wiley & Sons, Inc., ISBN 978-047-1354-04-8, New Jersey, USA

Zheltikov, A. M. (2006). Phase Coherence Control and Subcycle Transient Detection in Nonlinear Raman Scattering with Ultrashort Laser Pulses. *Physical Review A,* Vol 74, 053403 (1-7), ISSN 1050-2947

Zhu, S. Y. & Scully, M. O. (1996). Spectral Line Elimination and Spontaneous Emission Cancellation via Quantum Interference. *Physical Review Letters,* Vol 76, pp. 388-391, ISSN 0031-9007

Zhuang, F.; Shen, J. Q. & Ye, J. (2007). Controlling the Photonic Bandgap Structures via Manipulation of Refractive Index of Electromagnetically Induced Transparency Vapor. *Acta Physica Sinica (China),* Vol 56, pp. 541-545, ISSN 1000-3290

Photonic Crystals - Introduction, Applications and Theory
Edited by Dr. Alessandro Massaro

The first volume of the book concerns the introduction of photonic crystals and applications including design and modeling aspects. Photonic crystals are attractive optical materials for controlling and manipulating the flow of light. In particular, photonic crystals are of great interest for both fundamental and applied research, and the two dimensional ones are beginning to find commercial applications such as optical logic devices, micro electro-mechanical systems (MEMS), sensors. The first commercial products involving two-dimensionally periodic photonic crystals are already available in the form of photonic-crystal fibers, which use a microscale structure to confine light with radically different characteristics compared to conventional optical fiber for applications in nonlinear devices and guiding wavelengths. The goal of the first volume is to provide an overview about the listed issues.

How to reference
In order to correctly reference this scholarly work, feel free to copy and paste the following:

Teh-Chau Liau, Jin-Jei Wu, Jian Qi Shen and Tzong-Jer Yang (2012). EIT-Based Photonic Crystals and Photonic Logic Gate Design, Photonic Crystals - Introduction, Applications and Theory, Dr. Alessandro Massaro (Ed.), ISBN: 978-953-51-0431-5, InTech, Available from: http://www.intechopen.com/books/photonic-crystals-introduction-applications-and-theory/eit-based-photonic-crystals-and-photonic-logic-gate-design

INTECH
open science | open minds